HENRY
Hydraulic Engineering Repository

Ein Service der Bundesanstalt für Wasserbau

Conference Paper, Published Version

Yeh, Gour-Tsyh (George); Cheng, Hwai-Ping (Pearce); Cheng, Jing-Ru (Ruth) C.

Modeling Bay/Estuary Circulation with Method of Characteristics

Zur Verfügung gestellt in Kooperation mit/Provided in Cooperation with:
Kuratorium für Forschung im Küsteningenieurwesen (KFKI)

Verfügbar unter/Available at: https://hdl.handle.net/20.500.11970/109730

Vorgeschlagene Zitierweise/Suggested citation:
Yeh, Gour-Tsyh (George); Cheng, Hwai-Ping (Pearce); Cheng, Jing-Ru (Ruth) C. (2012): Modeling Bay/Estuary Circulation with Method of Characteristics. In: Hagen, S.; Chopra, M.; Madani, K.; Medeiros, S.; Wang, D. (Hg.): ICHE 2012. Proceedings of the 10th International Conference on Hydroscience & Engineering, November 4-8, 2012, Orlando, USA.

Standardnutzungsbedingungen/Terms of Use:

Die Dokumente in HENRY stehen unter der Creative Commons Lizenz CC BY 4.0, sofern keine abweichenden Nutzungsbedingungen getroffen wurden. Damit ist sowohl die kommerzielle Nutzung als auch das Teilen, die Weiterbearbeitung und Speicherung erlaubt. Das Verwenden und das Bearbeiten stehen unter der Bedingung der Namensnennung. Im Einzelfall kann eine restriktivere Lizenz gelten; dann gelten abweichend von den obigen Nutzungsbedingungen die in der dort genannten Lizenz gewährten Nutzungsrechte.

Documents in HENRY are made available under the Creative Commons License CC BY 4.0, if no other license is applicable. Under CC BY 4.0 commercial use and sharing, remixing, transforming, and building upon the material of the work is permitted. In some cases a different, more restrictive license may apply; if applicable the terms of the restrictive license will be binding.

MODELING BAY/ESTUARY CIRCULATION WITH METHOD OF CHARACTERISTICS

Gour-Tsyh (George) Yeh[1], Hwai-Ping (Pearce) Cheng[2], and Jing-Ru (Ruth) C. Cheng[3]

ABSTRACT

We present a numerical approach containing a splitting strategy, the method of characteristics (MOC), a backward particle tracking technique, and the Galerkin finite element method to solve two-dimensional depth-averaged shallow water flow equations which are commonly used to describe bay/estuary hydrodynamics. With the splitting strategy, we first employ the MOC to solve equations without the eddy flux terms. We specifically choose wave front propagation directions for the characteristic equations to perform local diagonalization. The characteristics form of the governing equation offers great advantages over the conservative form in adapting appropriate numerical algorithms and in defining boundary conditions. Innovative hyperbolic numerical algorithms can be employed to approximate the system because each of the three equations is a decoupled advective transport equation of a wave. The specification of boundary conditions is made easy pending the wave direction. The boundary condition for any wave is needed only when it is transported into the region of interest. When a wave is transported out of the region, there is no need to specify the boundary condition because internal flow dynamics due to this wave affects the boundary values of tide and velocity components. In other words, external world will not affect the wave that is transported out of the region. The Galerkin finite element method is applied to solve the Eulerian step of the Lagrangian-Eulerian form of equations. A standing wave problem was used to verify the accuracy and robustness of the approach. Two circulation problems at Salem Harbor and San Diego South Bay, respectively, were employed to demonstrate the application of the model.

1. INTRODUCTION

Shallow water equations are widely used to model bay/estuary circulation. In some cases, the equations can have exact solutions under simplifying assumptions [Ghosh and Debnath, 1997]. In practice, however, numerical solutions are needed to deal with complicated real-world systems. The rapid progress in the field of computer technology, the advancement of knowledge in numerical methods, and most importantly, the growing demand for reliable information on flows in bay/estuary areas have encouraged scientists and engineers to use numerical simulation techniques

[1] Graduate Institute of Applied Geology
National Central University, Jhongli, Taiwan
[2] ERDC, US Army Corps of Engineers, Vicksburg, MS, USA
[3] ERDC, US Army Corps of Engineers, Vicksburg, MS, USA

to solve steady/unsteady flow problems. Many numerical strategies have been presented to handle the governing equations where non-linearity is introduced due to the strong coupling between fluid depth and velocities. Some researchers constructed their strategies on the platform of the finite difference method [Shi and Toro, 1996; Fennema and Chaudhry, 1989], while others did on the finite element [Walters and Barragy, 1997; Petera and Nassehi, 1996] or the finite volume method [Zhou and Goodwill, 1997; Anastasiou and Chan, 1997]. The numerical strategies included total variation diminishing method [Tseng and Liang, 1997], two-step explicit method [Park et al., 1995], semi-implicit method [Cecchi et al., 1998], implicit method [Fennema and Chaudhry, 1989], high-order time integration scheme [Ozkan-Haller and Kirby, 1997], upwind/upstream numerical schemes [Shi and Toro, 1996; Anastasiou and Chan, 1997], filtered solution method [Laible and Lillys, 1997], least square method [Muccino et al, 1997; Tseng and Liang, 1997], method of characteristics [Lai, 1977; Hirsch et al., 1987], and hybrid Lagrangian-Eulerican method [Hansen and Arneborg, 1997; Petera and Nassehi, 1996]. Some numerical modelers have applied parallel as well as multigrid methods to improve computational efficiency [Spitaleri and Corinaldesi, 1997; Hinkelmann and Zielke, 1996].

Recently, the Lagrangian-Eulerian approach has attracted many numerical modelers' attention because it can avoid many types of numerical errors when advection/convection dominates [Yeh, 1990]. Casulli and Cheng have shown that the approach is unconditionally stable when it is used to solve one-dimensional (1-D) shallow water equations [Casulli and Cheng, 1990]. Petera and Nassehi employed a particle tracking technique in the Lagrangian step and have demonstrated their approach would provide very stable results for the convection dominated very shallow depth computation in estuaries [Petera and Nassehi, 1996].

The MOC might be considered the most appropriate way to solve wave or hyperbolic-type equations because it approaches problems not only mathematically but also physically. Lai has developed comprehensive MOC models to solve 1-D shallow water equations [Lai, 1987] and has incorporated the MOC with the finite difference discretization to solve 2-D flow equations [Lai, 1977]. In this study, we incorporate the MOC with the finite element discretization to solve two-dimensional (2-D) depth-averaged shallow water equations. When the MOC is used to solve 1-D equations (e.g., channel flow equations), diagonalization can be achieved easily [Abbott, 1966]. Its application to 2-D cases, however, is not straightforward [Hirsch et al., 1987]. The three characteristics associated with 2-D shallow water equations can be chosen in any direction [Lai, 1977]. Many iterations might be needed to reach convergence in the numerical simulation if the characteristic directions are not appropriately taken. To handle this, we perform local diagonalization for the 2-D characteristic equations. We also apply the Lagrangian approach to solve the characteristic equations, rather than the original governing equations, where a particle tracking technique [Cheng et al., 1996] is used to transport characteristic variables along characteristic lines. In the following sections, we will describe first the depth-averaged hydrodynamic mathematical model used to simulate bay/estuary circulation, followed by our numerical approach associated with the MOC to solve the governing equations. Finally, we will employ two examples to verify and to demonstrate our approach.

2. SHALLOW WATER WAVE EQUATION

The governing equations of two-dimensional circulation flow in the bay/estuary area can be described by shallow water equations which are derived based on the conservation law of water

mass and linear momentum and through the depth-averaging process [Wang and Connor, 1975] as follows

$$\begin{cases} \text{Continuity Equation:} \quad \dfrac{\partial h}{\partial t} + \nabla \cdot \left(\mathbf{V} h \right) = q \\ \text{Momentum Equation:} \\ \dfrac{\partial \mathbf{V}}{\partial t} + \nabla \cdot \left(\mathbf{V}\mathbf{V} \right) = -g\nabla h - g\nabla Z_o - \dfrac{\boldsymbol{\tau}^b}{\rho_o h} - f\mathbf{V} \times \mathbf{k} + \dfrac{\boldsymbol{\tau}^w}{\rho_o h} + \dfrac{1}{\rho_o} \nabla \cdot \boldsymbol{\tau} \\ \text{(1)} \quad \text{(2)} \quad \text{(3)} \quad \text{(4)} \quad \text{(5)} \quad \text{(6)} \quad \text{(7)} \quad \text{(8)} \\ \qquad + \dfrac{1}{\rho_o} \nabla \cdot \mathbf{R} - \dfrac{gh}{2\rho_o} \nabla \left(\Delta\rho \right) + g\nabla\zeta - \dfrac{1}{\rho_o} \nabla p_s \\ \qquad \text{(9)} \quad \text{(10)} \quad \text{(11)} \quad \text{(12)} \end{cases} \tag{1}$$

where h is the water depth, [L] (Figure 1); t is the time, [M]; $\mathbf{V}$ is the velocity vector, [L/T]; q is the source/sink flow rate due to artificial injection/withdraw, rainfall/evaporation, and exfiltration/infiltration from groundwater [L/T]; g is the gravitational constant, [L/T^2]; Z_o is the bottom elevation, [L]; $\boldsymbol{\tau}^b$ is the bottom shear stress [M/(LT^2)]; ρ_o is the reference density, [M/L^3]; f is the coriolis force parameter, [1/T]; $\mathbf{k}$ is the unit vector along the vertical direction, [dimensionless]; $\boldsymbol{\tau}^w$ is the surface wind stress, [M/(LT^2)]; $\boldsymbol{\tau}$ is the eddy stress, [M/(LT^2)]; $\mathbf{R}$ is the radiation stress due to short wave, [M/(LT^2)]; $\Delta\rho$ is the density deviation from its reference value, [M/L^3]; ζ is the astronomical tide, [L]; and p_s is the atmosphere pressure on the surface, [M/(LT^2)]. In general cases, all 12 terms in Eq. (1) must be included. However, in many occasions, only the terms marked with the red are included.

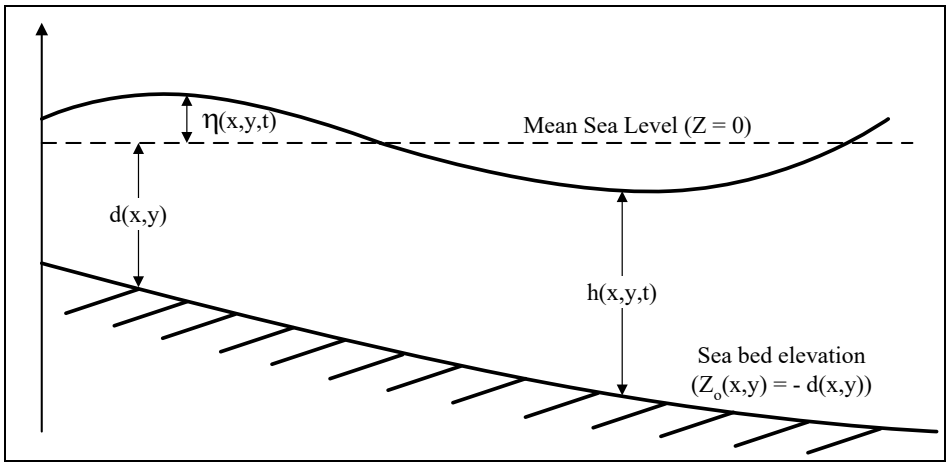

Figure 1 Definitions of tide η(x,y,t), water depth h(x,y,t), and sea bed elevation Z_o(x,y)

3. LOCAL DIAGONALIZATION

The governing equations for shallow water circulation and tides in the conservative form can be transformed into the wave form as follows (Yeh et al., 2000)

$$\begin{Bmatrix} \dfrac{\partial W_1}{\partial t}+u\dfrac{\partial W_1}{\partial x}+v\dfrac{\partial W_1}{\partial y} \\ \dfrac{\partial W_2}{\partial t}+\left(u+ck_x^{(2)}\right)\dfrac{\partial W_2}{\partial x}+\left(v+ck_y^{(2)}\right)\dfrac{\partial W_2}{\partial y} \\ \dfrac{\partial W_3}{\partial t}+\left(u-ck_x^{(2)}\right)\dfrac{\partial W_3}{\partial x}+\left(v-ck_y^{(2)}\right)\dfrac{\partial W_3}{\partial y} \end{Bmatrix}+\begin{Bmatrix} S_1 \\ S_2 \\ S_3 \end{Bmatrix}= \tag{2}$$

$$\begin{Bmatrix} A_1 \\ A_2 \\ A_3 \end{Bmatrix}-\begin{Bmatrix} G_1 \\ G_2 \\ G_3 \end{Bmatrix}+\begin{Bmatrix} \Gamma_1^w \\ \Gamma_2^w \\ \Gamma_3^w \end{Bmatrix}-\begin{Bmatrix} \Gamma_1^b \\ \Gamma_2^b \\ \Gamma_3^b \end{Bmatrix}+\begin{Bmatrix} D_1 \\ D_2 \\ D_3 \end{Bmatrix}-\begin{Bmatrix} T_1 \\ T_2 \\ T_3 \end{Bmatrix}+\begin{Bmatrix} R_1 \\ R_2 \\ R_3 \end{Bmatrix}-\begin{Bmatrix} C_1 \\ C_2 \\ C_3 \end{Bmatrix}-\begin{Bmatrix} B_1 \\ B_2 \\ B_3 \end{Bmatrix}$$

where W_1, W_2, and W_3 are three characteristic variables representing the shear, positive gravity, and negative gravity wave, respectively, [L/T], [T], and [T], respectively; u and v are the x- and y-velocity, respectively, [L/T]; $c=\sqrt{gh}$ is the is the wave celerity [L/T]; $h=Z_o+\eta$ is the water depth [L]; η is the tide elevation above mean sea level [L] (Figure 1); Z_o is the bottom elevation above a datum [L]; $k_x^{(2)}$ and $k_y^{(2)}$ are the x- and y -components, respectively, of the unit vector of the second wave propagation direction $\mathbf{k}^{(2)}$, [1]; $\{S_1,S_2,S_3\}^T$ is the coupling vector of three waves, [L/T^2], [1], and [1], respectively; $\{A_1,A_2,A_3\}^T$ is the artificial source sink of three waves, [L/T^2], [1], and [1], respectively; $\{G_1,G_2,G_3\}^T$ is the gravity force acting on three waves, [L/T^2], [1], and [1], respectively; $\{\Gamma_1^w,\Gamma_2^w,\Gamma_2^w\}^T$ is the wind stress acting on three waves, [L/T^2], [1], and [1], respectively; $\{\Gamma_1^b,\Gamma_2^b,\Gamma_2^b\}^T$ is the bottom shear stress acting on three waves, [L/T^2], [1], and [1], respectively; $\{D_1,D_2,D_3\}^T$ is the viscous diffusive force acting on three waves, [L/T^2], [1], and [1], respectively; $\{T_1,T_2,T_3\}^T$ is the astronomical tide acting on three waves, [L/T^2], [1], and [1], respectively; $\{R_1,R_2,R_3\}^T$ is the radiation short wave acting on three waves, [L/T^2], [1], and [1], respectively; $\{C_1,C_2,C_3\}^T$ is the coriolis force acting on three waves, [L/T^2], [1], and [1], respectively; and $\{B_1,B_2,B_3\}^T$ is the buoyancy force acting on three waves, [L/T^2], [1], and [1], respectively. These 10 vectors [$\{S_1,S_2,S_3\}^T$, $\{A_1,A_2,A_3\}^T$, $\{G_1,G_2,G_3\}^T$, $\{\Gamma_1^w,\Gamma_2^w,\Gamma_2^w\}^T$, $\{\Gamma_1^b,\Gamma_2^b,\Gamma_2^b\}^T$, $\{D_1,D_2,D_3\}^T$, $\{T_1,T_2,T_3\}^T$, $\{R_1,R_2,R_3\}^T$, $\{C_1,C_2,C_3\}^T$, and $\{S_1,S_2,S_3\}^T$] are defined as follows

$$\begin{Bmatrix} S_1 \\ S_2 \\ S_3 \end{Bmatrix} = \begin{Bmatrix} g\left(k_y^{(1)} \dfrac{\partial \eta}{\partial x} - k_x^{(1)} \dfrac{\partial \eta}{\partial yx} \right) \\ \dfrac{h}{c}\left[k_y^{(2)} k_y^{(2)} \dfrac{\partial u}{\partial x} + k_x^{(2)} k_x^{(2)} \dfrac{\partial v}{\partial y} - k_x^{(2)} k_y^{(2)} \left(\dfrac{\partial u}{\partial y} + \dfrac{\partial v}{\partial x} \right) \right] \\ \dfrac{-h}{c}\left[k_y^{(2)} k_y^{(2)} \dfrac{\partial u}{\partial x} + k_x^{(2)} k_x^{(2)} \dfrac{\partial v}{\partial y} - k_x^{(2)} k_y^{(2)} \left(\dfrac{\partial u}{\partial y} + \dfrac{\partial v}{\partial x} \right) \right] \end{Bmatrix} \tag{3}$$

$$\begin{bmatrix} \partial W_1 & A_1 & G_1 & \Gamma_1^w & \Gamma_1^b & D_1 & T_1 & R_1 & C_1 & B_1 \\ \partial W_2 & A_2 & G_2 & \Gamma_2^w & \Gamma_2^b & D_2 & T_2 & R_2 & C_2 & B_2 \\ \partial W_3 & A_3 & G_3 & \Gamma_3^w & \Gamma_3^b & D_3 & T_3 & R_3 & C_2 & B_3 \end{bmatrix} = \begin{bmatrix} 0 & k_y^{(1)} & -k_x^{(1)} \\ \dfrac{1}{c} & \dfrac{k_x^{(2)}}{g} & \dfrac{k_y^{(2)}}{g} \\ -\dfrac{1}{c} & \dfrac{k_x^{(2)}}{g} & \dfrac{k_y^{(2)}}{g} \end{bmatrix} \times$$

$$\begin{bmatrix} \partial \eta & q & u\dfrac{\partial Z_o}{\partial x} + v\dfrac{\partial Z_o}{\partial y} & 0 & 0 & 0 & 0 & 0 & 0 & 0 \\ \partial u & -\dfrac{qu}{h} & 0 & \dfrac{\tau_x^w}{\rho_o h} & \dfrac{\tau_x^b}{\rho_o h} & \dfrac{1}{\rho_o}\left(\dfrac{\partial \tau_{xx}}{\partial x} + \dfrac{\partial \tau_{xy}}{\partial y} \right) & g\dfrac{\partial \varsigma}{\partial x} & \dfrac{1}{\rho_o}\left(\dfrac{\partial R_{xx}}{\partial x} + \dfrac{\partial R_{xy}}{\partial y} \right) & fv & \dfrac{gh}{2\rho_o}\dfrac{\partial \Delta\rho}{\partial x} \\ \partial v & -\dfrac{qv}{h} & 0 & \dfrac{\tau_y^w}{\rho_o h} & \dfrac{\tau_y^b}{\rho_o h} & \dfrac{1}{\rho_o}\left(\dfrac{\partial \tau_{yx}}{\partial x} + \dfrac{\partial \tau_{yy}}{\partial y} \right) & g\dfrac{\partial \varsigma}{\partial y} & \dfrac{1}{\rho_o}\left(\dfrac{\partial R_{yx}}{\partial x} + \dfrac{\partial R_{yy}}{\partial y} \right) & -fu & \dfrac{gh}{2\rho_o}\dfrac{\partial \Delta\rho}{\partial y} \end{bmatrix} \tag{4}$$

where $k_x^{(1)}$ and $k_y^{(1)}$ are the x- and y-components, respectively, of the unit vector of the first wave propagation direction $\mathbf{k}^{(1)}$; τ_x^w and τ_y^w are the components of surface wind shear stress along the x- and y-directions, respectively, over unit horizontal overland area [M/L/T^2]; τ_x^b and τ_y^b are the components of bottom shear stress along the x- and y-directions over unit horizontal overland area [M/L/T^2]; τ_{xx} is the eddy stress in the x-direction on the plane perpendicular to x-direction [M/(LT^2)]; τ_{xy} is the eddy stress in the x-direction on the plane perpendicular to y-direction [M/(LT^2)]; τ_{yx} is the eddy stress in the y-direction on the plane perpendicular to x-direction [M/(LT^2)]; τ_{yy} is the eddy stress in the y-direction on the plane perpendicular to y-direction [M/(LT^2)]; ς is the astronomical tide, [L]; R_{xx} is the radiation stress due to short waves in the x-direction on the plane perpendicular to x-direction [M/(LT^2)]; R_{xy} is the radiation stress due to short waves in the x-direction on the plane perpendicular to y-direction [M/(LT^2)]; R_{yx} is the radiation stress due to short waves in the y-direction on the plane perpendicular to x-direction [M/(LT^2)]; and R_{yy} is the radiation stress due to short waves in the y-direction on the plane perpendicular to y-direction [M/(LT^2)].

It is clear from Eq. (3), we can choose $\mathbf{k}^{(1)}$ and $\mathbf{k}^{(2)}$ to make $\{S_1, S_2, S_3\}^T = \{0,0,0\}^T$ for a complete diagonalization of three wave equations in Eq. (2) by selecting $\mathbf{k}^{(1)}$ and $\mathbf{k}^{(2)}$ to satisfy the following equations

$$k_y^{(1)} \frac{\partial \eta}{\partial x} - k_x^{(1)} \frac{\partial \eta}{\partial y} = 0 \tag{5}$$

$$k_y^{(2)} k_y^{(2)} \frac{\partial u}{\partial x} + k_x^{(2)} k_x^{(2)} \frac{\partial v}{\partial y} - k_x^{(2)} k_y^{(2)} \left(\frac{\partial u}{\partial y} + \frac{\partial v}{\partial x} \right) k_y^{(1)} \frac{\partial \eta}{\partial x} - k_x^{(1)} \frac{\partial \eta}{\partial y} = 0 \tag{6}$$

We can always find $k_x^{(1)}$ and $k_y^{(1)}$ to satisfy Eq. (5), i.e., wave direction that is tangential to the gradient of tidal elevation can always be found. However, we will not be able to find any real solutions of $k_x^{(2)}$ and $k_y^{(2)}$ in solving Eq. (6) when the discriminant of the quadratic equation, i.e., $\left(\frac{\partial u}{\partial y} + \frac{\partial v}{\partial x} \right)^2 - 4 \frac{\partial u}{\partial x} \frac{\partial v}{\partial y}$ is less than zero. In this case, Hirsh et al. have suggested to select directions which minimize the coupling terms [Hirsh et al, 1987], e.g., S_2 and S_3 in our case here. Under such circumstances, we calculate $k_x^{(2)}$ and $k_y^{(2)}$ with the following equation [Hirsh et al, 1987]

$$\tan\left(\frac{2k_y^{(2)}}{k_x^{(2)}} \right) = \left(\frac{\partial u}{\partial y} + \frac{\partial v}{\partial x} \right) / \left(\frac{\partial u}{\partial x} - \frac{\partial v}{\partial y} \right) \tag{7}$$

It is noteworthy that by choosing wave decomposition with Eqs. (5) and (6) or Eqs. (5) and (7), it may be possible to decouple or minimize the coupling terms and obtain diagonalization of the shallow water equations. However, numerical experiments show that this approach often suffer from convergence problem [e.g., Paillere et al. 1998]. The characteristic directions are dependent on the numerical solution and sensitive to the accurate evaluation of the gradients of water depth and velocity components. Numerical stability and convergence are the major concern. When convergence becomes problematic, four other options are provided in the selection of $\mathbf{k}^{(1)}$ and $\mathbf{k}^{(2)}$ to overcome the problem. These are: Option 1, $\mathbf{k}^{(1)}$ and $\mathbf{k}^{(2)}$ are chosen arbitrary; Option 2, $\mathbf{k}^{(1)}$ and $\mathbf{k}^{(2)}$ are chosen along the Froude line [Paillere et al. 1998]; Option 3, $\mathbf{k}^{(1)}$ is obtained by Eq. (5) and $\mathbf{k}^{(2)}$ is chosen along the velocity; and Option 4, $\mathbf{k}^{(1)}$ is obtained by Eq. (5) and $\mathbf{k}^{(2)}$ is chosen to be along the opposite direction of $\mathbf{k}^{(1)}$ [Guinot, 2005]. Other ad hoc approaches of selecting $\mathbf{k}^{(2)}$ based on some geometric parameters are possible [Katopodes and Strelkoff 1978]. While the first characteristic direction can always be selected in the depth gradient direction, the second characteristic directions can be chosen arbitrary, for example, along the x-direction, the y-direction or the steepest elevation gradients. This approach may be less accurate and grid orientation of the numerical solutions may occur.

4. BOUNDARY CONDITIONS

In solving Equation (1), the water depth *h*, and the velocity components, *u* and *v*, must be given initially or they can be obtained by simulating the steady-state version of the conservative form of Eq. (1). In addition, appropriate boundary conditions need to be specified to match the corresponding physical system. The characteristics form of the governing equation offers great advantages over the conservative form in adapting appropriate numerical algorithms and in defining boundary conditions. Innovative hyperbolic numerical algorithms can be employed to approximate

the system because each of the three equations is a decoupled advective transport equation of a wave. The determination of the number of boundary conditions that consist with physics is not straightforward when the conservative form of equations is used. However, when the characteristic form of equations is used, the number of boundary conditions that conform to the physics can easily be determined. We demonstrate how boundary conditions are specified in the following. A boundary segment can be either open or closed. In the former case, the boundary condition for any wave is needed only when it is transported into the region of interest. When a wave is transported out of the region, there is no need to specify the boundary condition because internal flow dynamics due to this wave affects the boundary values of *u*, *v*, and *h*. In other words, external world will not affect the wave that is transported out of the region.

Open upstream boundary condition (At Open Boundaries during Flood Tide):

At an open upstream boundary segment, $\mathbf{n}\cdot\mathbf{V}<0$; thus the vorticity is always transported into the region from upstream. If $\mathbf{n}\cdot c\mathbf{k}^{(2)}<0$, then $-\mathbf{n}\cdot c\mathbf{k}^{(2)}>0$. Under such circumstance, $\mathbf{n}\cdot\left(\mathbf{V}+c\mathbf{k}^{(2)}\right)<0$ and $\mathbf{n}\cdot\left(\mathbf{V}-c\mathbf{k}^{(2)}\right)$ may be less than 0 or greater than 0; thus the positive gravity wave is transported into the region and the negative gravity wave may be transported into the region or out of the region. Similarly, If $\mathbf{n}\cdot c\mathbf{k}^{(2)}>0$, then $-\mathbf{n}\cdot c\mathbf{k}^{(2)}<0$. Under such circumstance, $\mathbf{n}\cdot\left(\mathbf{V}-c\mathbf{k}^{(2)}\right)<0$ and $\mathbf{n}\cdot\left(\mathbf{V}+c\mathbf{k}^{(2)}\right)$ may be less than 0 or greater than 0; thus the negative gravity wave is transported into the region and the positive gravity wave may be transported into the region or out of the region. If $\mathbf{n}\cdot c\mathbf{k}^{(2)}=0$, then all three waves are transported into the region.

Based on the above discussions, it is seen that at an upstream open boundary, either all three waves are transported into the region or two waves are transported into the region. Thus, either three boundary conditions or two boundary conditions are needed. When three boundary conditions are needed, they are given as follows

$$h=h^{(up)}(\mathbf{x}_b,t);\ u=u^{(up)}(\mathbf{x}_b,t);\ \text{and}\ v=v^{(up)}(\mathbf{x}_b,t) \tag{8}$$

where $h^{(up)}(\mathbf{x}_b,t)$, $u^{(up)}(\mathbf{x}_b,t)$ and $v^{(up)}(\mathbf{x}_b,t)$ being functions of the boundary coordinate $\mathbf{x}_b$ and time *t* are the water depth, x-component velocity, and y-component velocity, respectively, of the upstream incoming fluid. When two boundary conditions are needed, one of the boundary conditions is user's specified water depth, normal flux, or rating curve flux and the other would be obtained by assuming the tangential flux is zero. The third equation for the boundary condition would be either the positive gravity wave function or the negative gravity wave function. The three equations are mathematically stated as

$$\begin{aligned} &h=h^{(up)}(\mathbf{x}_b,t),\ \left(\mathbf{n}\cdot\mathbf{V}\right)h=q_n^{(up)}(\mathbf{x}_b,t),\ \text{or}\ \left(\mathbf{n}\cdot\mathbf{V}\right)h=q_r^{(up)}(h);\quad \left(\mathbf{l}\cdot\mathbf{V}\right)h=0;\\ &\text{and}\ F_+\left(u,v,h\right)=\Im_+\left(u_+^*,v_+^*,h_+^*\right)\ \text{or}\ F_-\left(u,v,h\right)=\Im_-\left(u_-^*,v_-^*,h_-^*\right) \end{aligned} \tag{9}$$

where $\mathbf{n}$ is the outward unit vector normal to the boundary; $q_n^{(up)}(\mathbf{x}_b,t)$, a function of the boundary coordinate $\mathbf{x}_b$ and time t, is the normal flux of the upstream incoming fluid; $q_r^{(up)}(h)$, a function of water depth h, is the rated flux at the upstream boundary; $\mathbf{l}$ is the unit vector tangential to the upstream boundary; $F_+\left(u,v,h\right)$, a function of *u*, *v*, and h, is the positive gravity wave function; $\Im_+\left(u_+^*,v_+^*,h_+^*\right)$ is the positive gravity wave forcing function of u_+^*, v_+^* and h_+^* in which u_+^*, v_+^* and h_+^*,

respectively, are the *x*-component of the velocity, the *y*-component of the velocity, and water depth at the root of positive gravity wave, respectively; $F_{-}(u,v,h)$, a function of u, v, and h. is the negative gravity wave function; and $\Im_{-}\left(u_{-}^{*},v_{-}^{*},h_{-}^{*}\right)$ is the negative gravity wave forcing function of u_{-}^{*}, v_{-}^{*} and h_{-}^{*} in which u_{-}^{*}, v_{-}^{*} and h_{-}^{*}, respectively, are the *x*-component of the velocity, the *y*-component of the velocity, and water depth at the root of positive gravity wave, respectively.

Open downstream boundary condition (At Open Boundaries during Ebb Tide):

At an open downstream boundary segment, $\mathbf{n}\cdot\mathbf{V}>0$; thus the vorticity is always transported out of the region from upstream. If $\mathbf{n}\cdot c\mathbf{k}^{(2)}>0$, then $-\mathbf{n}\cdot c\mathbf{k}^{(2)}<0$. Under such circumstance, $\mathbf{n}\cdot\left(\mathbf{V}+c\mathbf{k}^{(2)}\right)>0$ and $\mathbf{n}\cdot\left(\mathbf{V}-c\mathbf{k}^{(2)}\right)$ may be greater than 0 or less than 0; thus the positive gravity wave is transported out of the region and the negative gravity wave may be transported out of the region or into the region. Similarly, If $\mathbf{n}\cdot c\mathbf{k}^{(2)}<0$, then $-\mathbf{n}\cdot c\mathbf{k}^{(2)}>0$. Under such circumstance, $\mathbf{n}\cdot\left(\mathbf{V}-c\mathbf{k}^{(2)}\right)>0$ and $\mathbf{n}\cdot\left(\mathbf{V}+c\mathbf{k}^{(2)}\right)$ may be greater than 0 or less than 0; thus the negative gravity wave is transported out of the region and the positive gravity wave may be transported out of the region or into the region. If $\mathbf{n}\cdot c\mathbf{k}^{(2)}=0$, then all three waves are transported out of the region.

Based on the above discussions, it is seen that at a downstream open boundary, either all three waves are transported out of the region or only one wave is transported into the region. Thus, either no boundary condition or only one boundary condition is needed. When no boundary condition is needed, the three equations required for the downstream open boundary are obtained based on three wave functions as

$$\begin{aligned} &h=h^{(dn)}(\mathbf{x}_b,t)\text{ or }\left(\mathbf{n}\cdot\mathbf{V}\right)h=q_r^{(dn)}(h);\ F_{\otimes}\left(u,v,h\right)=\Im_{\otimes}\left(u_{\otimes}^{*},v_{\otimes}^{*},h_{\otimes}^{*}\right);\\ &\text{and }F_{-}\left(u,v,h\right)=\Im_{-}\left(u_{-}^{*},v_{-}^{*},h_{-}^{*}\right)\text{ or }F_{+}\left(u,v,h\right)=\Im_{+}\left(u_{+}^{*},v_{+}^{*},h_{+}^{*}\right)\end{aligned}\qquad(10)$$

where $h^{(dn)}(\mathbf{x}_b,t)$ and $q_r^{(dn)}(h)$ being functions of the boundary coordinate $\mathbf{x}_b$ and time t are the prescribed water depth and rating curve at the downstream boundary.

Closed upstream boundary condition (At Closed Boundaries during Ebb Tide):

At the closed upstream boundary, the normal flux must be zero, i.e., $\left[\left(\mathbf{n}\cdot\mathbf{V}\right)h\right]=0$. To satisfy this condition, three possibilities can occur: (1) both water depth and the normal component of the velocity are zero, (2) normal component of the velocity is zero and water depth is not zero, (3) water depth is zero and normal component of the velocity is not zero. For the *Possibility (1)*, all three waves are standing and no boundary condition is needed. The three boundary-condition equations are obtained with three wave functions. For *Possibility (2)*, the vorticity wave is standing and one of the gravity wave is transported out of the region while the other is transported into the region. Under such circumstance, only one boundary condition is required, which is the normal component of the velocity equal to zero itself. The other two boundary equations are obtained with the vorticity wave function and either the positive wave or the negative wave function. For *Possibility (3)*, all three waves are transported into the region; thus three boundary conditions must be prescribed: one is that the depth equal to zero and the other may be obtained by setting both normal and tangential components of the velocity equal to zero.

Based on the above description, the three equations to determine the water depth, x-component of the velocity, and y-component of the velocity for these possibilities are stated as follows

$$\begin{aligned}
&\textit{Possibility (1)}: F_{\otimes}\left(u,v,h\right)=\Im_{\otimes}\left(u^{(n)},v^{(n)},h^{(n)}\right);\ F_{+}\left(u,v,h\right)=\Im_{+}\left(u^{(n)},v^{(n)},h^{(n)}\right);\\
&\quad \text{and } F_{-}\left(u,v,h\right)=\Im_{-}\left(u^{(n)},v^{(n)},h^{(n)}\right)\\
&\textit{Possibility (2)}: \mathbf{n}\cdot\mathbf{V}=0;\ F_{\otimes}\left(u,v,h\right)=\Im_{\otimes}\left(u^{(n)},v^{(n)},h^{(n)}\right);\text{ and}\\
&\quad F_{+}\left(u,v,h\right)=\Im_{+}\left(u_{+}^{*},v_{+}^{*},h_{+}^{*}\right)\text{ or } F_{-}\left(u,v,h\right)=\Im_{-}\left(u_{-}^{*},v_{-}^{*},h_{-}^{*}\right)\\
&\textit{Possibility (3)}:\ h=0;\ \mathbf{n}\cdot\mathbf{V}=0;\ \text{and } \mathbf{l}\cdot\mathbf{V}=0
\end{aligned}\tag{11}$$

where $\Im_{\otimes}\left(u^{(n)},v^{(n)},h^{(n)}\right)$ is the vorticity wave forcing function of $u^{(n)}$, $v^{(n)}$ and $h^{(n)}$ in which $u^{(n)}$, $v^{(n)}$ and $h^{(n)}$, respectively, are the *x*-component of the velocity, the *y*-component of the velocity, and water depth at old time level n, respectively; $\Im_{+}\left(u^{(n)},v^{(n)},h^{(n)}\right)$ is the positive gravity wave forcing function of $u^{(n)}$, $v^{(n)}$ and $h^{(n)}$; and $\Im_{-}\left(u^{(n)},v^{(n)},h^{(n)}\right)$ is the negative wave forcing function of $u^{(n)}$, $v^{(n)}$ and $h^{(n)}$. It should be noted that for *Possibility (3)*, the rest of normal and tangential component of the velocity to zero implies that the boundary conditions will be switched to *Possibility (1)* in the next iteration.

Closed downstream boundary condition (At Closed Boundaries during Flood Tide):

At the closed downstream boundary, the flow rate must be zero. To satisfy this condition, three possibilities can occur: (1) water depth and the normal component of the velocity are zero, (2) the normal component of the velocity is zero and water depth is not zero, (3) water depth is zero and the normal component of the velocity is not zero. *For Possibility (1)*, all three waves are standing and no boundary condition is needed. The three boundary-condition equations are obtained with three wave functions. For *Possibility (2)*, the vorticity wave is standing and one of the two gravity waves is transported out of the region while the other is transported into the region. Under such circumstance, only one boundary condition is needed, which is the normal component of the velocity equal to zero itself. For *Possibility (3)*, all three waves are transported out of the region, no boundary condition is needed and the three boundary condition equations are obtained with three wave functions.

Based on the above description, the three equations to determine the water depth and velocity components for these possibilities are stated as follows

$$\begin{aligned}
&\textit{Possibility (1)}: F_{\otimes}\left(u,v,h\right)=\Im_{\otimes}\left(u^{(n)},v^{(n)},h^{(n)}\right);\ F_{+}\left(u,v,h\right)=\Im_{+}\left(u^{(n)},v^{(n)},h^{(n)}\right);\\
&\quad \text{and } F_{-}\left(u,v,h\right)=\Im_{-}\left(u^{(n)},v^{(n)},h^{(n)}\right)\\
&\textit{Possibility (2)}: \mathbf{n}\cdot\mathbf{V}=0;\ F_{\otimes}\left(u,v,h\right)=\Im_{\otimes}\left(u^{(n)},v^{(n)},h^{(n)}\right);\text{ and}\\
&\quad F_{+}\left(u,v,h\right)=\Im_{+}\left(u_{+}^{*},v_{+}^{*},h_{+}^{*}\right)\text{ or } F_{-}\left(u,v,h\right)=\Im_{-}\left(u_{-}^{*},v_{-}^{*},h_{-}^{*}\right)\\
&\textit{Possibility (3)}:\ F_{\otimes}\left(u,v,h\right)=\Im_{\otimes}\left(u_{\otimes}^{*},v_{\otimes}^{*},h_{\otimes}^{*}\right);\ F_{+}\left(u,v,h\right)=\Im_{+}\left(u_{+}^{*},v_{+}^{*},h_{+}^{*}\right);\\
&\quad \text{and } F_{-}\left(u,v,h\right)=\Im_{-}\left(u_{-}^{*},v_{-}^{*},h_{-}^{*}\right)
\end{aligned}\tag{12}$$

5. NUMERICAL APPROXIMATION

To provide robust and efficient numerical solutions of the governing equations, many options and strategies are provided in the present model so that a wide range of application-depending circumstances can be simulated. When the model is cast in conservative forms [Eq. (1)], the governing equations are discretized with the finite element method that satisfies the Ladzhenskaya-Bauska-Brezz (LBB) condition. When the model is cast in the decoupled wave form, the characteristic equations [Eq. (2)] are solved with the Lagrangian approach. To facilitate the implementation of boundary conditions, the Lagrangian approach is used to solve the primary unknowns on the boundary no matter which form of governing equations is adopted.
One of the key issues in the employment of Lagrangian approaches is the selection of the directions of characteristic waves. For one-dimensional problems, the selection is straightforward since there is only one direction. For two-dimensional problems, there are infinite directions but only two independent directions are needed to solve well-posed problems. Thus, the key in the Lagrangian step is the selection of these two directions. Five options are provided in the present model: (1) both angles are specified by users, (2) first angle is along the gradient of the pressure and second angle is along the velocity, (3) first angle is along the gradient of the pressure and second angle is by diagonalization of the two gravity waves, (4) first angle is along the gradient of the pressure and second angle is other side of unite circle [Guinot, 2005], and (5) both first and second angles are along the Froude line [Paillere et al. 1998]. When a convergent solution is achieved, all five options yield almost identical simulations. However, for some problems, some of these options have difficulties in achieving convergent solutions. These issues have been addressed elsewhere [Huang, 2006] and will not be repeated here

6. EXAMPLE PROBLEMS

Three example problems are presented to demonstrate the successful implementation of the splitting algorithm in the diagonalized wave equations. One is presented to verify the model. The other two are given to demonstrate the application of the model to real world problems.

6.1 Verification Problem

We used a one-dimensional standing wave example [Wang and Connor, 1975] to verify our approach. This problem was governed by the wave equations as follows

$$\frac{\partial^2 u}{\partial t^2} = c^2 \frac{\partial^2 u}{\partial x^2}; \quad \frac{\partial^2 \eta}{\partial t^2} = c^2 \frac{\partial^2 \eta}{\partial x^2}; \quad c^2 = gh \tag{13}$$

where u is the velocity along the flow direction [L/T]; c is the wave speed [L/T]; h is water depth [L]; η is the tide elevation above the mean sea level [L]; g is gravity [L/T^2]. The domain of interest was 200 m long in the x-direction and 50 m wide in the y-direction. It was discretized with 20 elements: 10 m x 50 m each. The mean water depth was 4 meters. The boundary end at $x = 200$ m was closed, while the other one at $x = 0$ m was open and the water surface elevation fluctuated up and down according to

$$\eta\big|_{x=0} = \eta_o \sin\left(\frac{2\pi t}{200}\right) \tag{14}$$

where η_o represents the amplitude of the sinusoidal surface deviation applied to the boundary $x = 0$ m. Therefore, we set $u = 0$ m/s at $x = 200$ m to satisfy boundary condition for the simulation. The analytical solution of this linear wave problem is as follows

$$\begin{aligned} u &= -\frac{\eta_o \sqrt{c}}{h\cos\left(\frac{2\pi}{\sqrt{c}}\right)} \sin\left[\frac{2\pi}{\sqrt{c}}\left(\frac{x}{200}-1\right)\right]\cos\left(\frac{2\pi t}{200}\right) \\ \eta &= \frac{\eta_o \sqrt{c}}{\cos\left(\frac{2\pi}{\sqrt{c}}\right)} \cos\left[\frac{2\pi}{\sqrt{c}}\left(\frac{x}{200}-1\right)\right]\sin\left(\frac{2\pi t}{200}\right) \end{aligned} \tag{15}$$

Given initial condition at $t = 50$ s according to Eq. (14), we first chose $\eta_o = 0.1$ in this example to perform a simulation of 400 seconds, i.e., from $t = 50$ s to $t = 450$ s. We found the numerical solution was essentially unchanged for time step size less than 2.5 seconds and element number more than 20, which means we have obtained a grid convergent solution to the hydrodynamic flow equation (i.e., Eq. (2)) subject to the prescribed boundary condition. Figures 2 and 3 depict the numerical results and the analytical solutions of the tide elevation above mean sea level at $x = 100$ m and $x = 200$ m, respectively for $\eta_o =$ 0.1, 0.05, and 0.025. The differences between the numerical result and the analytical solution of Eq. (2) ((Figures 2(a) and 3(a)) was caused by the nonlinear terms accounted for in Eq. (2) but not in Eq. (13). To prove this, we reduced η_o from 0.1 to 0.05 and 0.025 to diminish the nonlinear effect. It is obvious that the difference decreased with the reduction of η_o. When η_o was reduced to 0.025, we had the computational result and the analytical solution match almost precisely (Figures 2(c) and 3(c)). An excellent agreement was also obtained in comparison of the velocity at time equal to 100 s, 200 s, 300 s, and 400 s for the case of $\eta_o = 0.025$ (Figure 4). It is thus verified that our MOC numerical model can solve standing wave problems accurately

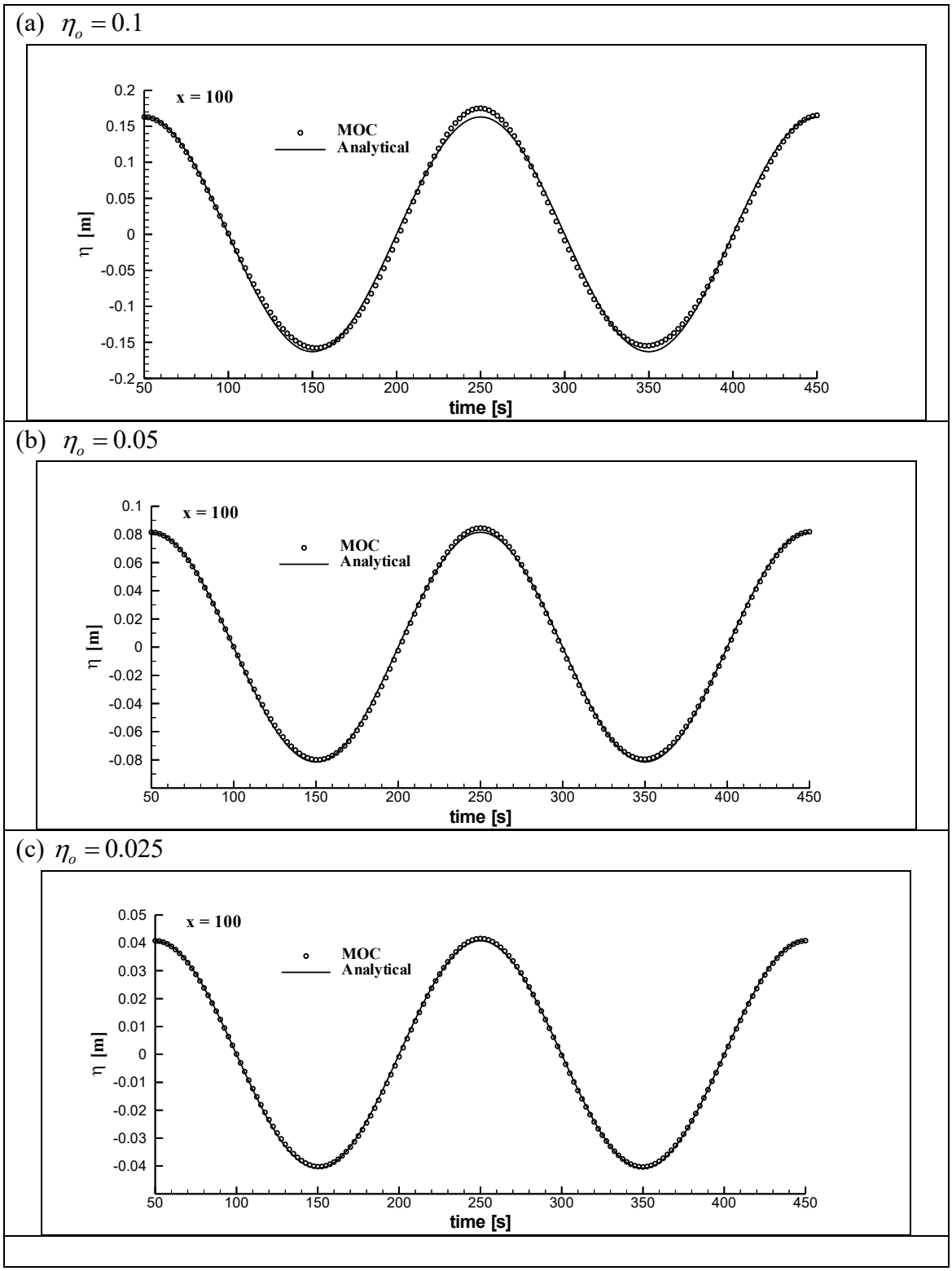

Figure 2 The tide elevation above mean sea level at $x = 100$ m for (a) $\eta_o = 0.1$ m, (b) $\eta_o = 0.05$ m, and (c) $\eta_o = 0.025$ m

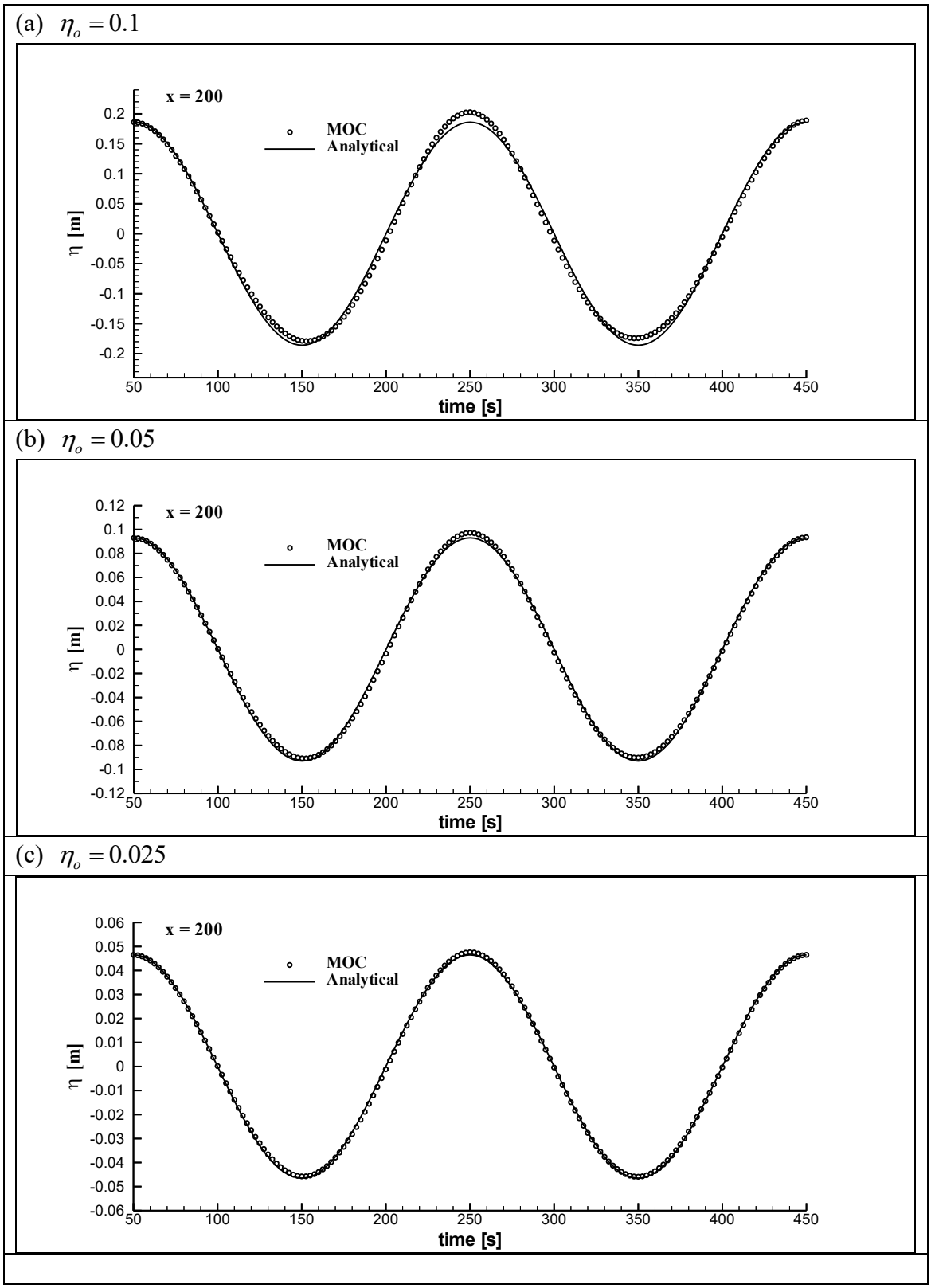

Figure 3 The tide elevation above mean sea level $x = 200$ m for (a) $\eta_o = 0.1$ m, (b) $\eta_o = 0.05$ m, and (c) $\eta_o = 0.025$ m

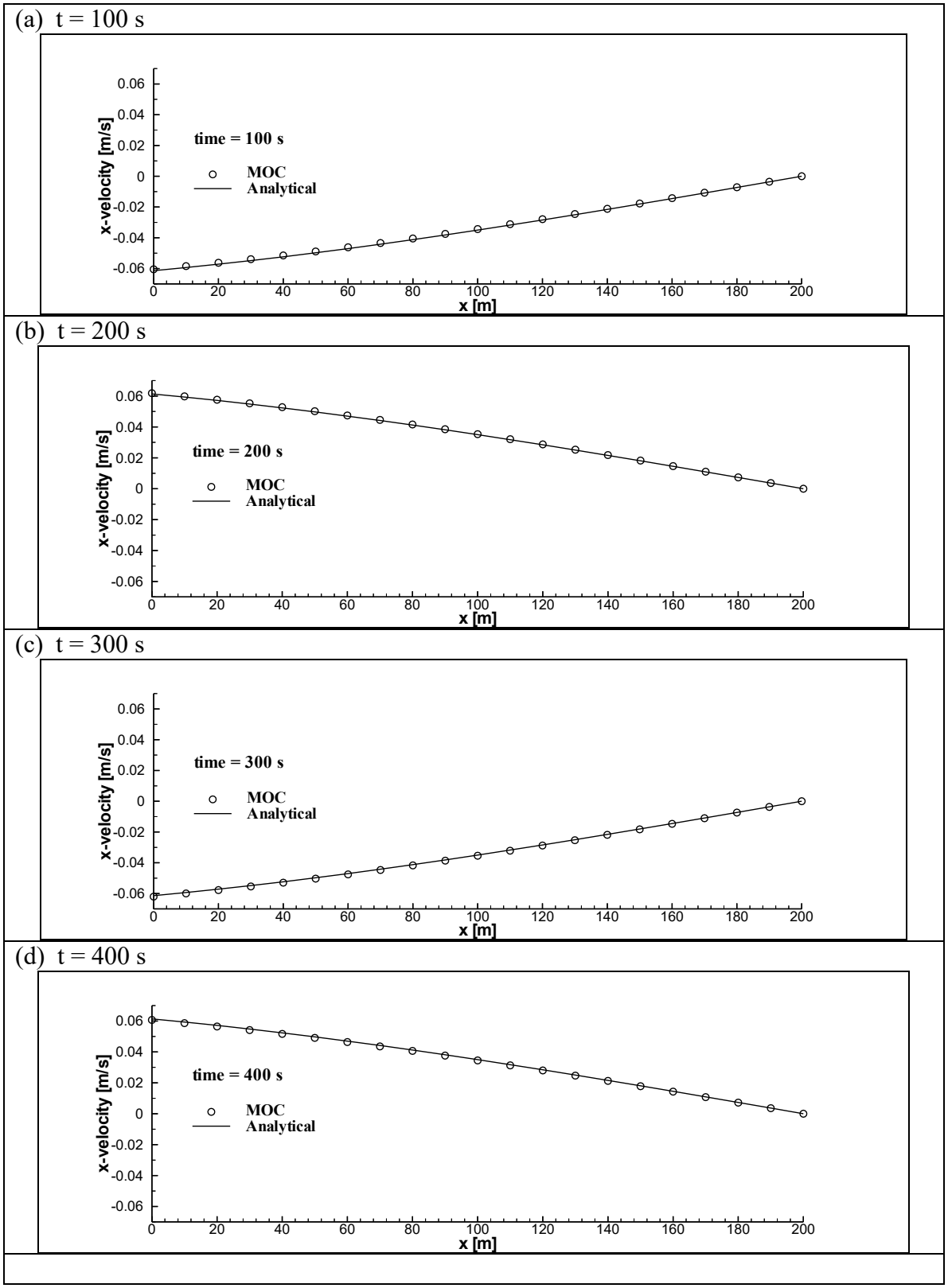

Figure 4 Comparison of analytical and numerical x-velocity at various times

6.2 Salem Harbor Problem

In this example, we used our model to determine water surface elevation at Salem Harbor [Yeh and Kalasinsky, 1977] where a tidal boundary condition was given on the open boundary side (i.e., x = 5,640 m, Figure 5(a)) and the closed boundary condition was employed at the other boundary sides. Twenty semidiurnal tidal cycles were applied, which made a 10 day simulation. The time step size was 20 seconds through the simulation. The maximum amplitude of the tide was 1.4 m. The eddy viscosity was assumed negligible. The tidal elevation was at zero initially. The domain was discretized with 275 nodes and 462 triangular elements (Figure 5(a)). The initial water depth varied from 1.4 m to 9.0 m (Figure 5(b)). Convergence was considered reached when either the maximum relative error of water depth was less than 10^{-4} or the root mean square error was less than 10^{-8}.

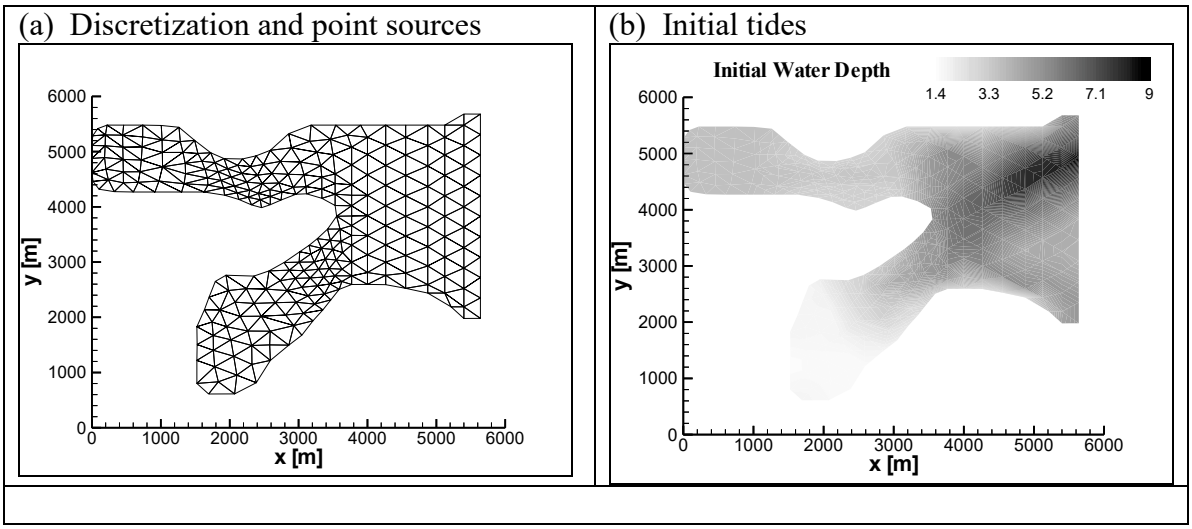

Figure 5 (a) Discretization and point sources and (b) Initial tides at Salem Harbor

Figures 6 and 7 plot the velocities and tidal elevations at T/4, T/2, 3T/4, and T during the twentieth tidal cycle where T denotes the time period of a tidal cycle. Based on the computational results, though not shown here, a quasi-steady flow pattern has been reached after three tidal cycles. In other words, this quasi-steady flow pattern repeated over and over after it is reached. The quasi-steady pattern was determined by comparing water depths of two consecutive tidal cycles at corresponding times. In this case we considered a quasi-steady flow to be reached when the maximum deviation of tidal elevation was less than 1 cm.

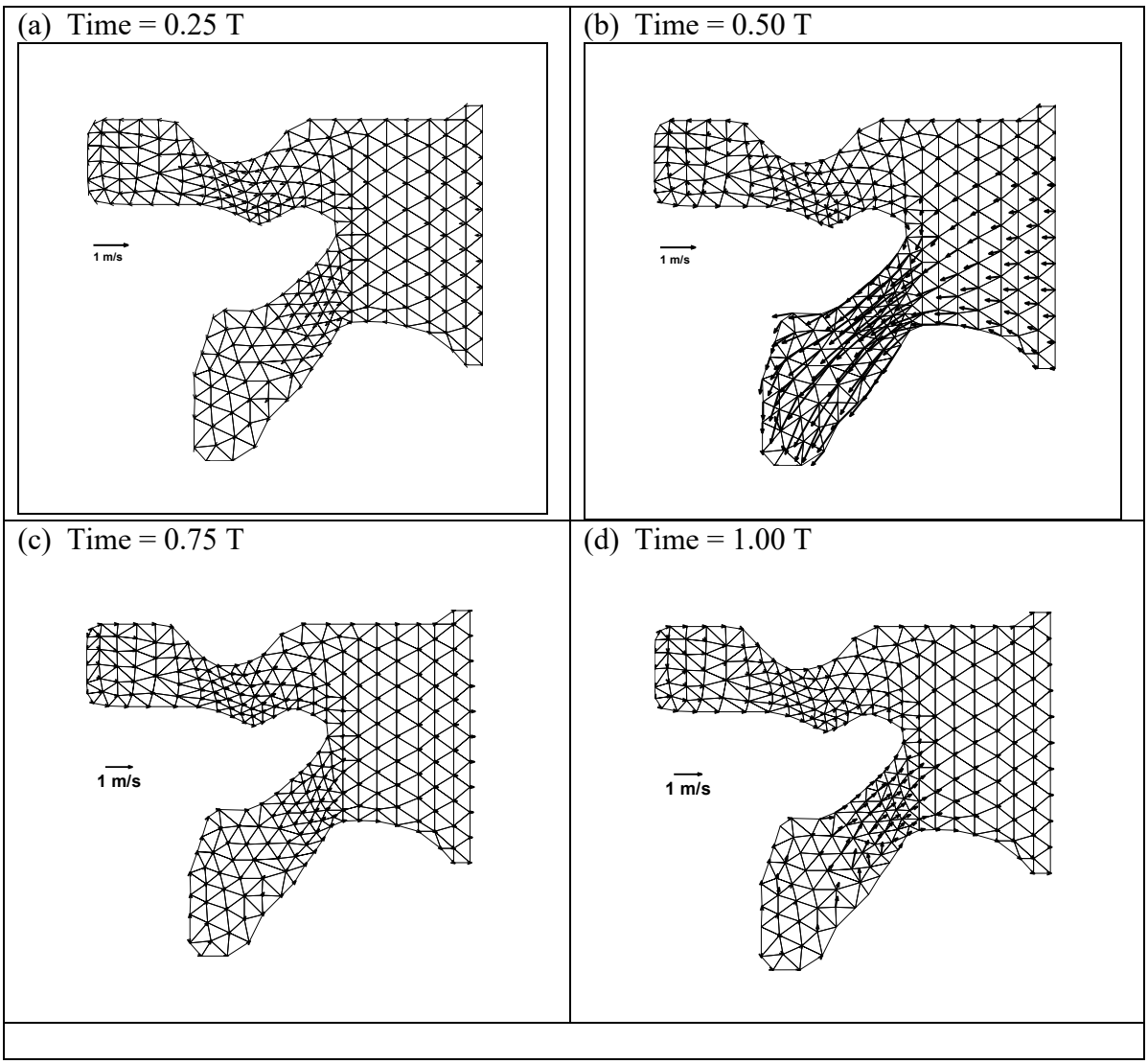

Figure 6 Velocity plot at various times of the twentieth tidal cycle, T = Tidal period

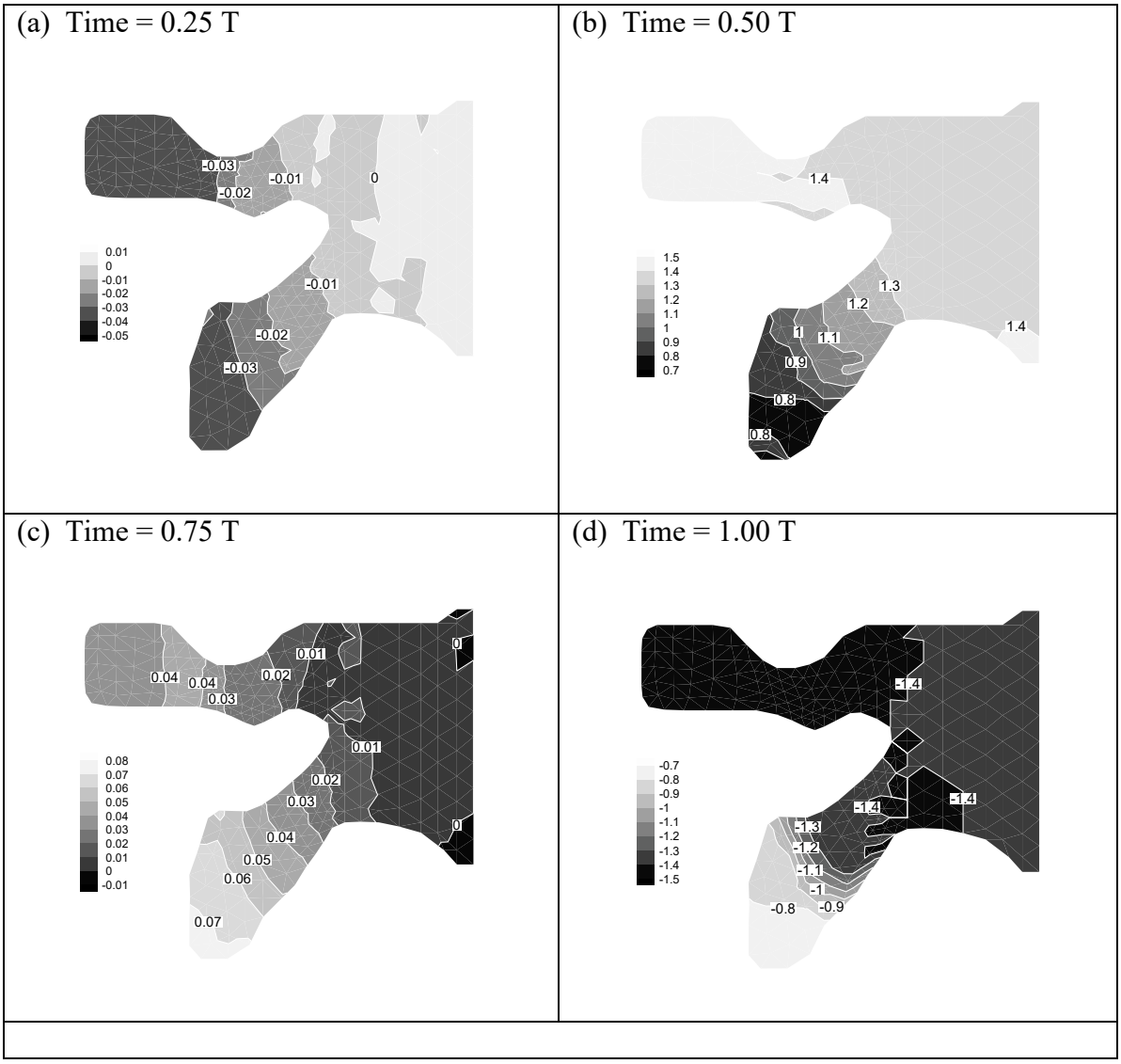

Figure 7 Tidal contour at various times of the twentieth tidal cycle, T = Tidal period

6.3 San Diego South Bay Problem

In this example, we used our model to simulate a hypothetical hydrodynamics at San Diego South Bay until a quasi-steady flow pattern reached. This quasi-steady flow pattern was computed with a hydrodynamic flow model which solved shallow water equations with time marching [Yeh et al., 2000]. The domain was discretized with 1,415 elements and 1,567 nodes (Figure 8). The mean depth varied from 20 meters near the ocean boundary to about 0.4 meter toward the south end of the bay. The flow pattern was determined with a tidal boundary condition implemented on the ocean boundary side where the maximum tidal amplitude was 1.2 m and with the rest of the boundary treated as closed (Figure 8). It was also assumed subject to 8 point sources (Figure 8) each with an injection rate of 1 m^3/s. Manning's n was assumed 0.01 throughout the entire bay. Figure 9 depicts the contours of water surface elevation in the bay area at various times during one tidal cycle.

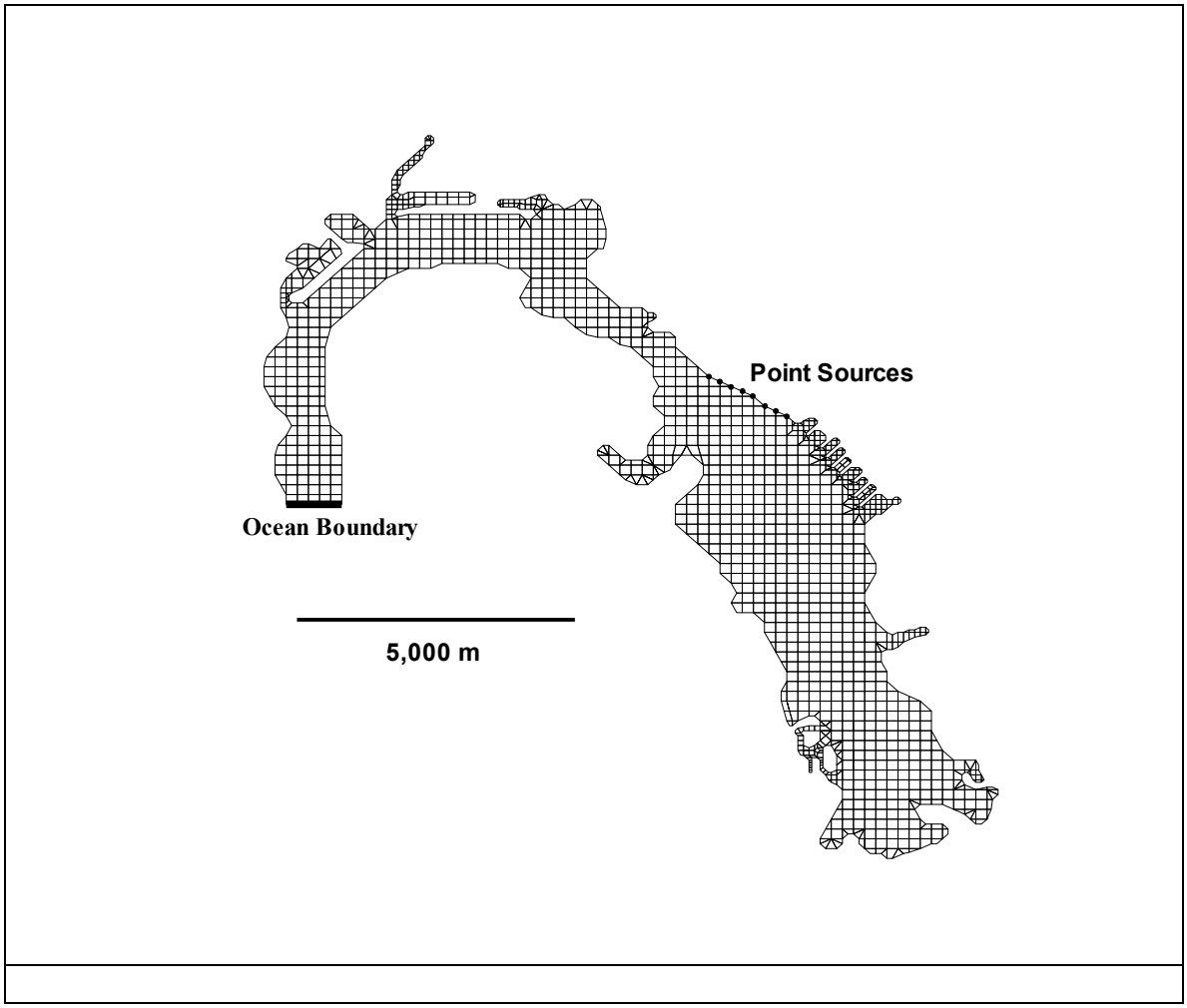

Figure 8 The domain and its discretization of San Diego South Bay

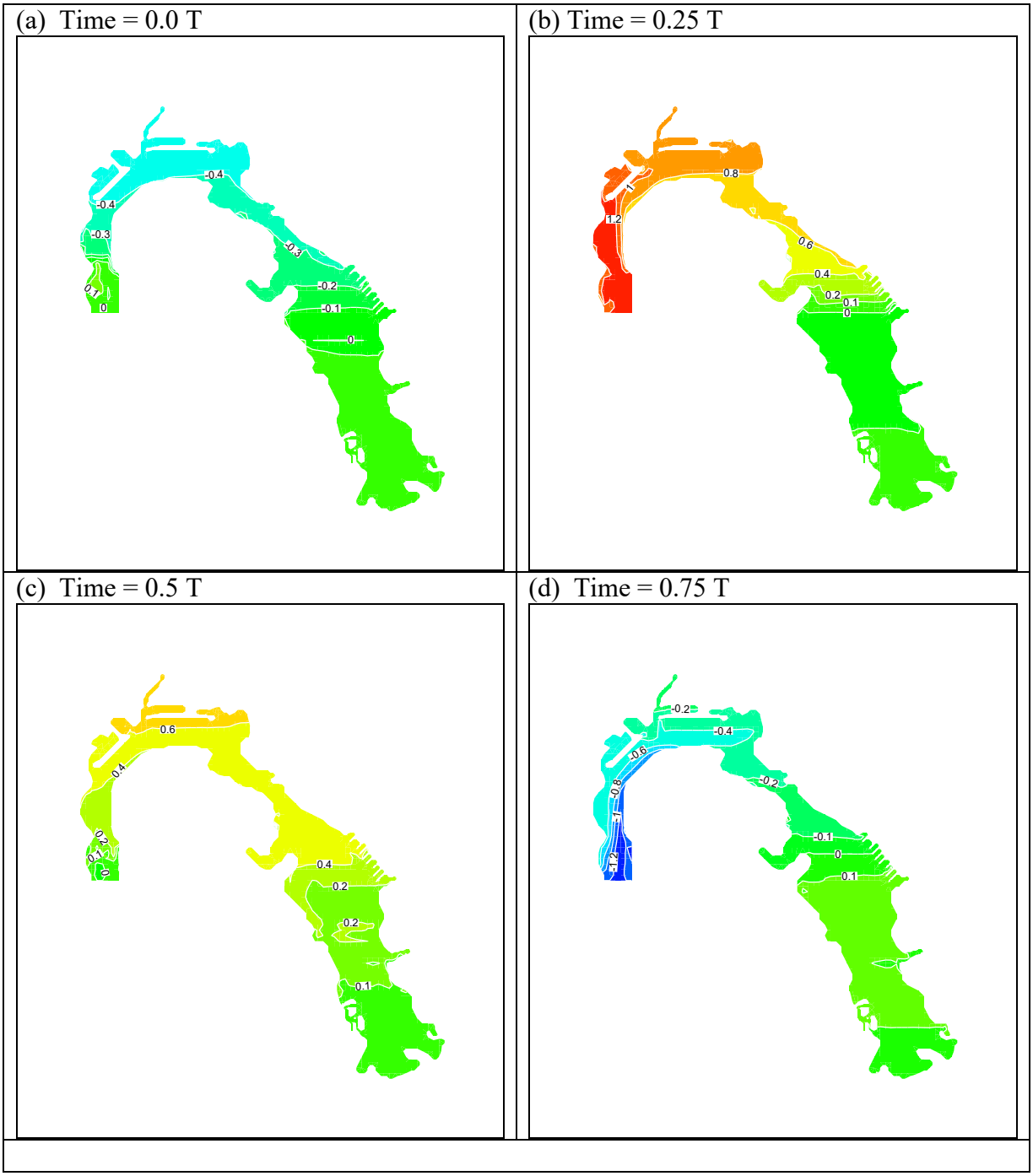

Figure 9 Tidal contour at various times of a tidal cycle at San Diego South Bay
T = Tidal period

The quasi steady state hydrodynamics including tides and currents provides the flow field to drive sediment, thermal, salinity, and water quality transport. Transient simulations of these scalor transport are beyond the scope of this paper. Sediment and water quality transport in San Diego South Bay are treated in a technical report by Yeh et al. (2000).

7. SUMMARY

A splitting strategy is employed in to solve two-dimensional shallow water equations which is used to describe circulation in the bay/estuary area. In this approach, we have used the method of characteristics first to solve the equations without including eddy flux terms, and then we accounted for these terms with the Galerkin finite element method. We may achieve local diagonalization by choosing two characteristic directions to make the coupling term of three waves zero. The cast of conservative form of shallow water equations in characteristic form greatly facilitates the implementation of boundary conditions. On open boundaries, either three boundary conditions or two boundary conditions are needed during flood tides while either no boundary condition or only one boundary condition is needed during ebb tides. On closed boundaries, the implementation of boundary conditions is much more involved than conventionally prescribed zero flux conditions. The implementation of these complicated boundary conditions at closed boundaries are discussed in great detail in this paper. Three examples were used to demonstrate the model. The one-dimensional standing wave problem was solved to verify the accuracy and efficiency of the present approach. Two field scale problems were employed to demonstrate the feasibility of using the method of characteristics to solve shallow water equations: one is the application to Salem Harbor and the other is to San Diego South Bay.

ACKNOWLEDGEMENT

This research is supported by National Science Council under Contract No. NSC 100-2811-M-008-67 with National Central University.

REFERENCES

Abbott, M. B., 1966, An introduction to the method of characteristics, American Elsevier, 243p.

Anastasiou, K and C. T. Chan, 1997, Solution of the 2D shallow water equations using the finite volume method on unstructured triangular meshes, International Journal for Numerical Methods in Fluids, 24(11), 1225-1245.

Casulli, V. and R. T. Cheng, 1990, Stability analysis of Eulerian-Lagrangian methods for the one-dimensional shallow-water equations, Applied Mathematical Modelling, 14(3), 122-131.

Cecchi, M. M., A. Pica, and E. Secco, 1998, Projection method for shallow water equations, International Journal for Numerical Methods in Fluids, 27(special issue), 81-95.

Cheng, H. P., J. R. Cheng, and G. T. Yeh, 1996, A particle tracking technique for the Lagrangian-Eulerian finite element method in multi-dimensions. International Journal for Numerical Methods in Engineering, 39(7), 1115-1136.

Chow, V. T, 1973, Open channel hydraulics, McGraw-Hill, 680p.

Fennema, J. F. and M. H. Chaudhry, 1989, Implicit methods for two-dimensional unsteady free-surface flows, Journal of Hydraulic Research, 27(3), 321-332.

Ghosh, K. K. and L. Debnath, 1997, Some exact solutions of non-linear shallow water equations, International Journal of Non-Linear Mechanics, 32(3), 633-636.

Guinot V. (2005). An approximate two-dimensional Riemann solver for hyperbolic systems of conservation laws. Journal of Computational Physics, Volume 205, Issue 1, p. 292-314.

Hansen, E. A. and L. Arneborg, 1997, Use of a discrete vortex model for shallow water flow around islands and coastal structures, Coastal Engineering, 32(2), 223-246.

Hinkelmann, R. and W. Zielke, 1996, Parallel three-dimensional Lagrangian-Eulerian model for the shallow water and transport equations, Proceedings for the 11th International Conference on Computational Methods in Water Resources, CMWR 96, v 2, 71-78.

Hirsch, Ch., C. Lacor, and H. Deconinck, 1987, Convection algorithms based on a diagonalization procedure for the multidimensional Euler equations, AIAA Journal, Vol. 25, 667-676.

Katopodes N., T. Strelkoff. (1979) Two-dimensional shallow-water wave models, J. Eng. Mech. Div., ASCE 105 (1979) 317–334.

Lai, C., 1987, Comprehensive method of characteristics models for flow simulation, J. of Hydraulic Engineering, 114(9), 1074-1097.

Lai, C., 1977, Computer simulation of two-dimensional unsteady flows in estuaries and embayments by the method of characteristics basic theory and the formulation of the numerical method, Report USGS Water-Resources Investigations 77-85, Reston, MA, USA.

Laible, J. P. and T. P. Lillys, 1997, A filtered solution of the primitive shallow-water equations, Advances in Water Resources, 20(1), 23-35.

Muccino, J. C., W. G. Gray, and M. G. G. Foreman, 1997, Calculation of vertical velocity in three-dimensional, shallow water equation, finite element models, International Journal for Numerical Methods in Fluids, 25(7), 779-802.

Ozkan-Haller, H. T. and J. T. Kirby, 1997, Fourier-Chebyshev collocation method for the shallow water equations including shoreline runup, Applied Ocean Research, 19(1), 21-34.

Paillère H., G. Degrez, H. Deconinck (1998). Multidimensional upwind schemes for the shallow water equations, International Journal for Numerical Methods in Fluids, Volume 26, Issue 8 , Pages 987 – 1000.

Park, S. S., K. F. Najjar, and C. G. Uchrin, 1995, Water quality management model for the lakes bay estuarine embayment 2: hydrodynamic tidal model, Journal of Environmental Science and Health, Part A: Environmental Science and Engineering & Toxic and Hazardous Substance Control, 30(5), 1077-1204.

Petera, J. and V. Nassehi, 1996, New two-dimensional finite element model for the shallow water equations using a lagrangian framework constructed along fluid particle trajectories, International Journal for Numerical Methods in Engineering, 39(24), 4159-4182.

Shi, J. and E. F. Toro, 1996, Fully discrete high-order shock-capturing numerical schemes, International Journal for Numerical Methods in Fluids, 23(3), 241-269.

Spitaleri, R. M. and L. Corinaldesi, 1997, Multigrid semi-implicit finite difference method for the two-dimensional shallow water equations, International Journal for Numerical Methods in Fluids, 25(11), 1229-1240.

Tseng, M. H. and S.-J. Liang, 1997, Comparison of second-order accurate TVD scheme and p-version space-time least-squares finite-element method for nonlinear hyperbolic problems, HPC Asia'97 Proceedings for the 2nd High Performance Computing on the Information Superhighway, 289-294.International Journal for Numerical Methods in Fluids, 24(1), 61-79.

Walters, R. A. and E. J. Barragy, 1997, Comparison of H and P finite element approximations of the shallow water equations, International Journal for Numerical Methods in Fluids, 24(1), 61-79.

Wang, J. D. and J. J. Connor, 1975, Mathematical modeling of near coastal circulation, Report MITSG 75-13, Massachusetts Institute of Technology, MA, USA.

Yeh, G. T., 1990, A Lagrangian-Eulerian method with zoomable hidden fine-mesh approach to solving advection-dispersion equations, Water Resources Research, 26(6), 1133-1144.

Yeh, G. T. and C. Kalasinsky, 1977, A two-dimensional finite element circulation model (CAFE), Report EN-139, Stone & Webster, Boston, MA, USA.

Yeh, G. T., H. P. Cheng, and J. R. Cheng, 2000. BEST: A Numerical Model to Simulate Bay/Estuarine Hydrodynamics and Sediment-chemical Transport. IN Schneider, J. M., 2000. A Shipyard Program for NPDES Compliance. Technical Memorandum. File No. 00-178. Applied Research Laboratory, The Pennsylvania State University, University Park, PA 16804.

Zhou, J. G. and I. M. Goodwill, 1997, Finite volume method for steady state 2-D shallow water flows, International Journal of Numerical Methods for Heat and Fluid Flow, 7(1), 4-23.